

LETTER

Iron isotope exchange kinetics at the nanoparticulate ferrihydrite surface

REBECCA L. POULSON, CLARK M. JOHNSON,* AND BRIAN L. BEARD

Department of Geology and Geophysics, University of Wisconsin, Madison, Wisconsin 53703, U.S.A.

ABSTRACT

The extent and rate of Fe-isotope exchange between aqueous Fe(III) atoms and those at the nanoparticulate ferrihydrite surface have been constrained using a ^{57}Fe -isotope tracer approach. Isotopic exchange was determined between hexaquo Fe(III) and 3 nm ferrihydrite under conditions analogous to natural environments at the equilibrium solubility of nanoparticulate ferrihydrite. Within approximately 11 days, the percent Fe-isotope (atom) exchange increased to a maximum of $26 \pm 5\%$, and remained constant within error over the remaining 12-week time of the experiment, suggesting that Fe-isotope exchange is limited to Fe atoms in available surface sites. These results confirm earlier work that used NTA- and EDTA-bearing solutions, which concluded isotopic exchange is largely limited to Fe at surface sites. Our results, however, which were obtained in dilute aqueous solutions at the natural solubility of 0.12 ppm aqueous Fe(III) (pH = 4.7), demonstrate that isotopic exchange rates are one to two orders of magnitude slower in the absence of $\text{Fe(III)}_{\text{aq}}$ -complexing ligands.

INTRODUCTION

Research into the material properties of nanoparticles (<100 nm) has seen growing interest in recent years. Particles in the nanometer size range are ubiquitous in nature, and their occurrence ranges from ultra-fine mineral dust in the atmosphere to nanocrystalline initial precipitates in the hydrosphere (e.g., Hochella 2002). Although it is increasingly recognized that the physical and thermodynamic properties of small particles may differ from those of larger particles (e.g., Ganguly et al. 1994), the extent of these variations in the nanodomain is known for relatively few materials. For example, various properties in the mineral hawleyite ($\beta\text{-CdS}$) have been observed empirically to change dramatically between the nanoscale and larger particle sizes. The properties of nanoscale $\beta\text{-CdS}$, relative to micrometer-sized and larger particles, include a fourfold decrease in melting temperature (Goldstein et al. 1992) and a factor of 4 increase in the pressure at which the tetrahedral to octahedral coordination transition occurs (Tolbert and Alivisatos 1995). These dramatic contrasts reflect the differences in particles at the nanoscale relative to those at the micrometer or larger scale. Additionally, because of the substantial increases in surface area that occur with decreasing size, a significant proportion of atoms in nanoparticles occur near the surface, markedly changing the reactivity of nanoparticles (Trudeau and Ying 1996).

Quantification of surface reactivity in nanoparticles has remained relatively unexplored. Most work has focused on changes in material properties at the nanoscale that have direct industrial and environmental applications, including the electronic properties of semiconductor nanomaterials (e.g., Waychunas 2001; Hochella 2002) and the mechanical and magnetic properties of nanoparticulate industrial catalysts (e.g., Trudeau and Ying 1996). Research into the surfaces of nanomaterials has been aimed primarily at understanding the bonding characteristics of atoms in surface sites (e.g., Zhao et al. 1994; Manceau and Gates

1997), but such studies do not directly assess surface reactivity. The nanoparticulate ferrihydrite (3 nm) selected for the present experimental work is ideal for investigating surface reactivity, given its increased surface area to volume ratio as a function of its reduced particle size.

Ferrihydrite is a naturally occurring nanoparticulate Fe^{3+} hydroxide that is commonly produced by oxidation of aqueous Fe(II) solutions at neutral pH. With time, nanoparticulate ferrihydrite grains tend to aggregate and coarsen to >100 nm-sized particles (Cornell and Schwertmann 1996). Long-term aging of ferrihydrite produces different Fe oxides, including goethite, lepidocrocite, hematite, or magnetite, depending on environmental conditions such as pH, temperature, and the chemical composition of ambient fluids. Understanding the surface reactivity of ferrihydrite is therefore important to studies of Fe oxide mineralogy of sediments, and surface reactivity also plays a critical role in sorption of numerous environmental contaminants (e.g., Stipp et al. 2002). Attenuation or release of toxic metals in groundwater systems is also controlled by the reactivity of ferrihydrite. Understanding the rates, magnitude, and mechanisms of exchange of nanoparticulate ferrihydrite is important for studies of Fe^{3+} oxy/hydroxides in natural environments.

We anticipate that isotopic exchange at room temperatures will be largely limited to surface atoms because of the very slow solid-state diffusion of Fe in minerals at low temperatures. Although solid-state diffusion is relatively rapid at high temperatures, where, for example, at 800 °C complete Fe exchange in 1 μm magnetite would be expected to occur in 10^{-3} to 1 year (Freer and Hauptman 1978), extrapolation of this diffusion rate to low temperatures suggests very long isotopic equilibration times even for nanometer-sized crystals, > 10^{15} years. Although there is uncertainty in extrapolation of a single diffusion coefficient to low temperatures, it serves to illustrate that solid-state diffusion at low temperatures will occur at very slow rates (if at all), presumably longer than the geologic timescales over which diagenetic alterations in ferrihydrite would occur.

* E-mail: clarkj@geology.wisc.edu

Here we use enriched stable-isotope tracers to directly quantify atom exchange between hexaquo aqueous Fe(III) and 3 nm ferrihydrite in terms of extent and rate. Use of stable-isotope tracers, followed by high-precision isotope-ratio mass spectrometry, offers a method of determining atom exchange that in principle is significantly more precise than that available using radioactive tracers and counting methods.

The findings of this study represent a first look at the exchangeability of Fe atoms on and off the ferrihydrite surface, independent of precipitation/dissolution or adsorption reactions. The extent of this exchange may be unique to ferrihydrite at the nanoscale, or this reactivity may be consistent throughout larger particle sizes, and further experimental work is warranted. If natural ferrihydrites experience Fe-atom exchange comparable to that observed in these nanoparticulate experiments, the Fe-isotope compositions of ferrihydrite samples in the presence of aqueous Fe (e.g., hydrothermal systems) may be altered by exchange—a potential effect that requires assessment.

EXPERIMENTAL DETAILS

Ferrihydrite

This study used a 3 nm-sized ferric oxyhydroxide ($\text{FeOOH}\cdot x\text{H}_2\text{O}$), or ferrihydrite, manufactured by Mach I Inc. This material has been studied by a variety of researchers in regard to its magnetic viscosity (Ibrahim et al. 1995), magnetism and spin dynamics (Ibrahim et al. 1994), agglomeration and phase transition (Feng et al. 1993), anomalous recoilless fraction (Ganguly et al. 1994), and structure and surface-bonding characteristics (Zhao et al. 1993, 1994). This ferrihydrite falls within the 2–15 nm size range usually reported for natural and synthetic 2-line ferrihydrite (5–6 nm most commonly observed by transmission electron microscopy) (Cornell and Schwertmann 1996). The manufacturer reported a surface area of $250 \text{ m}^2/\text{g}$ for this nanoparticulate ferrihydrite, and our own BET (Brunauer-Emmett-Teller) surface area analysis (by N_2 adsorption) yielded a surface area of $224 \pm 11 \text{ m}^2/\text{g}$; both values lie within the 200–400 m^2/g surface area range reported for natural and synthetic 2-line ferrihydrite by Cornell and Schwertmann (1996). Assuming a 3 nm-size spherical particle and a 2 Å surface layer (equivalent to the O-Fe bond distance; Zhao et al. 1993), roughly one-third of the Fe atoms in the ferrihydrite used may be considered to lie on the surface.

Zhao et al. (1993, 1994) obtained X-ray absorption spectra [both extended fine-structure (EXAFS) and near-edge (XANES)] on the same material used in this study, as well as laboratory synthesized 2-line ferrihydrite, and in both materials they measured changes in pre-edge peak areas that suggested 20–30% of the Fe atoms had bond lengths and coordinations that were significantly different than the octahedrally coordinated Fe of the bulk structure. These uniquely bonded Fe atoms were interpreted to be surface atoms that are tetrahedrally coordinated by four O atoms or OH groups. Manceau and Gates (1997) challenged the interpretations of Zhao et al. (1993, 1994), however, and instead suggested that the pre-peak intensities reflect distortions of surface Fe octahedra due to dehydration. Nevertheless, it seems clear that Fe atoms that lie closest to the surface in ferrihydrite sit in structural sites that are distinct from those of the bulk structure, and there is agreement that these atoms comprise 20–30% of the total Fe inventory in ferrihydrite. We infer, therefore, that these Fe atoms represent the most reactive Fe pool for isotopic exchange.

Aqueous Fe(III)

The isotopic tracer used in this study was a ^{57}Fe -enriched Fe(III) solution that had a ^{57}Fe abundance of 92.1%, as compared to the ferrihydrite, which had a natural ^{57}Fe abundance of 2.1% (see Appendix 1¹). For the experimental conditions of

this study ($\text{pH} = 4.7$, 25°C), the concentration of the ^{57}Fe spike solution was kept at the solubility of the aqueous Fe(III)-ferrihydrite system, as determined for the specific ferrihydrite used in this study. Weak HNO_3 was added to 2 L of ultrapure H_2O to achieve a pH of 4.7, and the 3 nm sized ferrihydrite was added in a 100 μM suspension, then aged several weeks. Because nitrate is a very weak ligand, all Fe(III) existed as $[\text{Fe}(\text{III})(\text{H}_2\text{O})_6]^{3+}$ (Skulan et al. 2002). A 1000 molecular weight cut-off (MWCO) dialysis membrane was immersed in the suspension, and the concentration of aqueous Fe(III) was measured from within the membrane over time, ensuring exclusion of any particulate ferrihydrite contaminant from aqueous samples. $\text{Fe}(\text{III})_{\text{aq}}$ contents remained constant between 7 and 33 days in two solubility runs within the uncertainty of the *Ferrozine* (Stookey 1970) analyses (Table 1), producing an average solubility of $0.11 \pm 0.03 \text{ ppm Fe}(\text{III})_{\text{aq}}$, which is essentially identical to that determined by Fox (1988) at $\text{pH} = 4.7$ (Fig. 1).

We stress that it was critical that the enriched ^{57}Fe -tracer experiments were conducted under conditions of chemical equilibrium so that no net mass transfer occurred through significant dissolution or precipitation. Under such equilibrium conditions, changes in Fe-isotope composition reflect only isotopic (atom) exchange. If, for example, the ^{57}Fe -enriched solution was oversaturated in aqueous Fe(III), ^{57}Fe -enriched Fe would be precipitated, resulting in an underestimate of the amount of exchange. Conversely, if undersaturated, dissolution of isotopically “normal” ferrihydrite would lower the measured $^{57}\text{Fe}/^{56}\text{Fe}$ ratio of aqueous Fe(III), and erroneously large amounts of isotopic exchange would be calculated. It is important to note that although running the experiments at solubility ensures that

TABLE 1. Solubility determination for 3 nm ferrihydrite

	Time (days)	Total Fe measured in aliquot (μg)	Initial aliquot volume (mL)	$\text{Fe}(\text{III})_{\text{aq}}$ (ppm)
Solubility Test 1	8	1.75	20	0.09
	14	2.04	20	0.10
Solubility Test 2	7	0.51	5	0.10
	15	0.80	5	0.16
	33	0.51	5	0.10

Notes: Iron contents measured by *Ferrozine* analysis (Stookey 1970) for aliquots of aqueous Fe in equilibrium with an aged 100 μM ferrihydrite suspension ($\text{pH} = 4.7$, 25°C). Aliquots were extracted from inside a 1000 MWCO dialysis membrane suspended within the ferrihydrite slurry, ensuring the exclusion of any particulate ferrihydrite contaminant from aqueous samples. A pH of 4.7 was confirmed for all solutions. Large aliquots (5 and 20 mL) were extracted from within the membrane and dried down prior to analysis, to concentrate the Fe such that *Ferrozine* analyses would fall in the ppm range. The average solubility of Fe measured in a saturated ferrihydrite suspension at $\text{pH} = 4.7$ was $0.11 \pm 0.03 \text{ ppm}$. Under these experimental conditions, all aqueous Fe was hexaquo Fe(III).

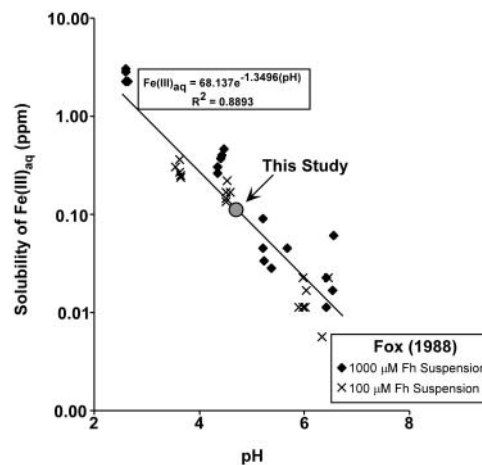


FIGURE 1. Solubility of aqueous Fe(III) in solutions (log-scale) supersaturated with colloidal ferric hydroxide (ferrihydrite; Fh) as a function of pH. Regression line and small symbols from Fox (1988). Results from this study (using a 100 μM Fh suspension made from 3 nm Fh) indicate a solubility of $0.11 \pm 0.03 \text{ ppm Fe}(\text{III})_{\text{aq}}$ (Table 1), which is identical within error to the value determined by Fox (1988) at $0.12 \pm 0.04 \text{ ppm Fe}(\text{III})_{\text{aq}}$ at $\text{pH} = 4.7$.

¹For a copy of the supplemental table, document item AM-05-015, contact the Business Office of the Mineralogical Society of America (see inside front cover of recent issue) for price information. Deposit items may also be available on the American Mineralogist web site (<http://www.minsocam.org> or current web address).

no net dissolution or precipitation occurs, in principle, dissolution/re-precipitation may remain a mechanism for isotopic exchange.

To ensure that the ^{57}Fe -enriched spike solution was at the equilibrium solubility concentration prior to addition of the ferrihydrite, 2 L of a slightly oversaturated (0.3 ppm) ^{57}Fe -enriched aqueous Fe(III) solution at pH = 4.7 (25 °C) was allowed to age at least one week, which induced some ferrihydrite precipitation, followed by removal of a 40 mL aliquot, ultracentrifugation, and sampling of the top 20 mL for use in each slurry. The total Fe_{aq} [effectively Fe(III) $_{\text{aq}}$] concentrations of these solutions were confirmed by *Ferrozine* (Stookey 1970) and graphite furnace atomic absorption spectrometry (AAS) analyses, which determined a total Fe_{aq} concentration of 0.12 ± 0.04 ppm for the ^{57}Fe spike solution, well within the range for Fe solubility noted above. The precipitated ferrihydrite was discarded. We note that for our experiments, it was important to approach equilibrium solubility from a slightly over-saturated solution to be certain that no net dissolution occurs, which would mistakenly over-estimate isotopic exchange.

Experimental procedure

The experiment used 17 low-density polyethylene bottles, each producing a specific time point, which contained 1–3 mg of ferrihydrite suspended in 20 mL of the aged 0.12 ppm ^{57}Fe -enriched Fe(III) $_{\text{aq}}$ solution. These bottles were placed on an orbital shaker and maintained at 25 °C, the same temperature at which the solubility experiments were run; samples were insulated from the orbital shaker to avoid temperature increases from heat produced by the shaker motor. Solution pH was monitored with pH-specific paper (± 0.2) and remained constant at 4.7 over the duration of the experiment. No pH buffer was added, because of the concern that additional ligands could affect the extent and rate of Fe-isotope exchange.

At each time point, one of the bottles was removed from the shaker and the pH was raised to ~ 7 through base addition (NH_4OH) to neutralize surface charges on the ferrihydrite and promote flocculation, followed by immediate removal of 1.6 mL aliquots for ultracentrifugation. Because of the very small size of the ferrihydrite, complete separation by ultracentrifugation was not possible, and residual ferrihydrite crystals in the aqueous Fe(III) aliquot produced artificially low $^{57}\text{Fe}/^{56}\text{Fe}$ ratios in the aqueous fraction, which would then over-estimate the percentage of isotopic exchange. The amount of contamination in the aqueous fraction by residual ferrihydrite crystals after centrifugation was calculated based on the measured Fe contents of the aqueous fraction relative to that expected based on our solubility determinations (see above). Although the wt% ferrihydrite contamination in the 1.6 mL aliquots is very low, between 10^{-4} and $10^{-7}\%$ (Appendix Table 1¹), indicating relatively efficient separation of ferrihydrite from solution, the molar percent contamination is significant due to the very low Fe(III) $_{\text{aq}}$ contents. The mol% contamination mode (e.g., most commonly measured value) for all aliquots analyzed ($n = 96$) was 86%, although there was a wide range (Fig. 2).

The measured $^{57}\text{Fe}/^{56}\text{Fe}$ ratios reflect a mixture between Fe(III) $_{\text{aq}}$ that has undergone isotopic exchange and Fe that reflects physical contamination by ferrihydrite. These mixing relations may be described through a series of percent isotopic exchange isopleths on a $^{57}\text{Fe}/^{56}\text{Fe}$ -mol% contamination diagram, several examples of which are illustrated in Figure 3. The percent exchange isopleths were calculated from standard “isotope dilution” mixing equations (e.g., Faure 1986) where, ideally, aliquots from a single time point bottle should plot along a single isopleth (Fig. 3A). Data from several bottles, however, plot along horizontal or sub-horizontal lines that are not parallel to the percent exchange isopleths (e.g.,

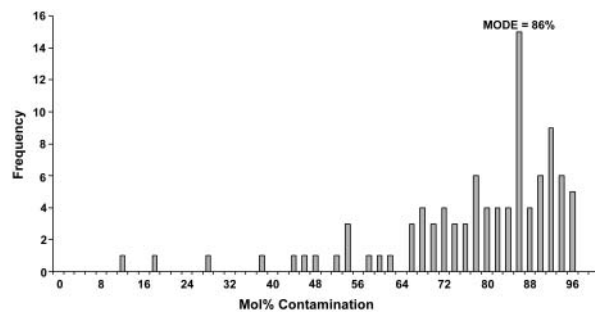


FIGURE 2. Histogram of molar percent of ferrihydrite contamination in the Fe(III) $_{\text{aq}}$ component for all individual aliquots ($n = 96$). The mol% contamination mode (e.g., most commonly measured value) is 86%. The asymmetric tail in the histogram to low mol% contamination is interpreted to reflect Fe loss during sample processing.

Fig. 3B); these trends probably reflect Fe loss during sample processing, which would produce anomalously low molar percent contamination values. We suspect that Fe loss occurred during evaporation of the very small Fe samples during processing. For nine out of seventeen bottles that produced low-angle molar percent contamination- $^{57}\text{Fe}/^{56}\text{Fe}$ trends, we assume a uniform molar percent contamination of 86% (Fig. 2) when calculating the percentage of isotopic exchange. Finally, in six bottles, more than half of the measured data cluster at a molar percent contamination that is higher than 86% (e.g., Fig. 3C), and in these cases, the measured percentage of contamination for aliquots $>86\%$ was used in determining the percentage of isotopic exchange. We recognize that the corrections discussed above will add some scatter to the calculated percentage of isotopic exchange, but such corrections

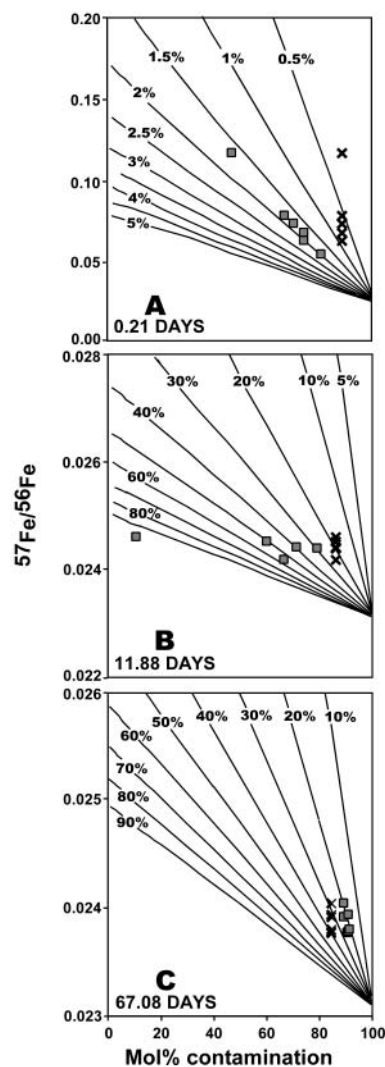


FIGURE 3. Plots of $^{57}\text{Fe}/^{56}\text{Fe}$ vs. mol% ferrihydrite contamination. Isopleths show the variation in $^{57}\text{Fe}/^{56}\text{Fe}$ as a function of mol% contamination at varying percents (as labeled) of Fe-isotope exchange (see Appendix 1 for details of calculation). Individual $^{57}\text{Fe}/^{56}\text{Fe}$ ratios (squares) are aliquots plotted against the measured mol% contamination; crosses show data corrected to a uniform 86% contamination (see text for discussion). The individual panels illustrate three different cases where (A) measured $^{57}\text{Fe}/^{56}\text{Fe}$ ratios and mol% contamination trend as expected along a single percentage exchange isopleth, (B) a horizontal or sub-horizontal trend of $^{57}\text{Fe}/^{56}\text{Fe}$ ratios vs. mol% contamination is interpreted to reflect Fe loss prior to analysis, and (C) measured molar percent contamination exceeds that of the modal 86% value. Analytical errors are smaller than symbol sizes used.

are necessary given the 10^3 molar contrast between the $\text{Fe(III)}_{\text{aq}}$ and ferrihydrite components and the sensitivity of even minute amounts of ferrihydrite contamination in the aqueous component.

Iron-isotope compositions, expressed as $^{57}\text{Fe}/^{56}\text{Fe}$ ratios, were determined on a GV Instruments *IsoProbe* following the methods of Beard et al. (2003), with the exception that a small-volume, water-cooled cyclonic spray chamber was used with an Elemental Scientific low-flow nebulizer (100 $\mu\text{L}/\text{min}$). This arrangement produces negligible memory between samples, which is important due to the wide ranges in isotopic compositions; desolvating nebulizers (e.g., *Aridus* by CETAC) can have significant memory effects. We also report Fe-isotope compositions as $\delta^{57/56}\text{Fe}$ values, which is the per mil (‰) deviation of a sample in $^{57}\text{Fe}/^{56}\text{Fe}$ relative to bulk Earth (Skulan et al. 2002). Measured Fe-isotope compositions were corrected for instrumental mass bias based on measurements of a known ultrapure standard every fourth analysis. External precision may be estimated from multiple analyses of standards (distinct from those used for mass-bias corrections) of known isotopic compositions at varying concentrations run throughout each analytical session. The long-term reproducibility in $^{57}\text{Fe}/^{56}\text{Fe}$ ratios for 34 standards is $\pm 4.6 \times 10^{-5}$ (1σ), which is equivalent to $\pm 2.0\text{‰}$ in $\delta^{57/56}\text{Fe}$ units; this relatively large error reflects the small quantity of Fe available for analysis (see Appendix 1). An uncertainty of 2.0‰ in the $^{57}\text{Fe}/^{56}\text{Fe}$ ratio will introduce an uncertainty of only 1% in the calculated percentage of isotopic exchange at 26% exchange.

Iron was measured directly and was not processed through ion-exchange chromatography. Iron contents in the solutions were measured during mass analysis, as calculated relative to reference solutions of varying concentration, and these contents were used to calculate the mol% ferrihydrite contamination in the aqueous Fe(III) component. Precision of the Fe concentration measurements can be estimated from multiple analyses of a 1 ppm ultrapure standard; reproducibility for 34 analyses is ± 0.05 ppm, which corresponds to an average error in calculated mol% ferrihydrite contamination of $\pm 1\%$. (See Appendix 1 for a tabulation of all Fe-isotope data and methods used to calculate the percentage of isotopic exchange.)

RESULTS AND DISCUSSION

Isotopic exchange increased during the first 11 days, and remained constant at $26 \pm 5\%$ over the remaining duration of the 83-day experiment (Fig. 4). The percentage of isotope exchange vs. time relations can be used to infer the kinetics of exchange between aqueous Fe(III) atoms and those at the ferrihydrite surface. The data from this study can be fit by two distinct rates. Using data from the first 12 days, the amount of

isotope exchange can be approximated with a reaction rate of $0.00081 \pm 0.00003/\text{h}$, assuming a first-order rate law (Fig. 4). For the remainder of the experiment, there was no change in the amount of isotope exchange, and a best-fit line to the data is a horizontal line (Fig. 4). The fact that the percentage of isotope exchange as a function of time is best fit by two curves, one with a positive slope, and the other by a horizontal line, suggests that all isotope exchange takes place by a single mechanism, followed by cessation of exchange. Because the extent of isotopic exchange over the long term lies within the 20–30% estimate for the proportion of distorted surface Fe sites in the ferrihydrite as inferred by Zhao et al. (1993, 1994) based on XANES and EXAFS spectra, we suggest that isotope exchange occurred at these labile surface sites. Moreover, because the data that define a positive correlation between percentage of exchange and time

TABLE 2. Percent isotopic exchange

Bottle	Days	% Exchange	
		Average	1-SD
1	0.04	0.3	0.1
2	0.21	2	0.1
3	3.1	5	2
4	11.0	21	4
5	11.9	20	3
6	16.0	23	2
7	21.0	29	4
8	22.1	35	2
9	27.1	26	11
10	31.9	23	2
11	35.0	23	4
12	41.0	28	3
13	45.8	30	7
14	46.7	29	3
15	67.1	21	2
16	70.0	35	8
17	83.1	24	5

Note: Average % isotopic exchange and associated 1σ errors for each experimental time point as determined from the $^{57}\text{Fe}/^{56}\text{Fe}$ ratios and mol% ferrihydrite contamination of individual aliquots (Appendix Table 1).

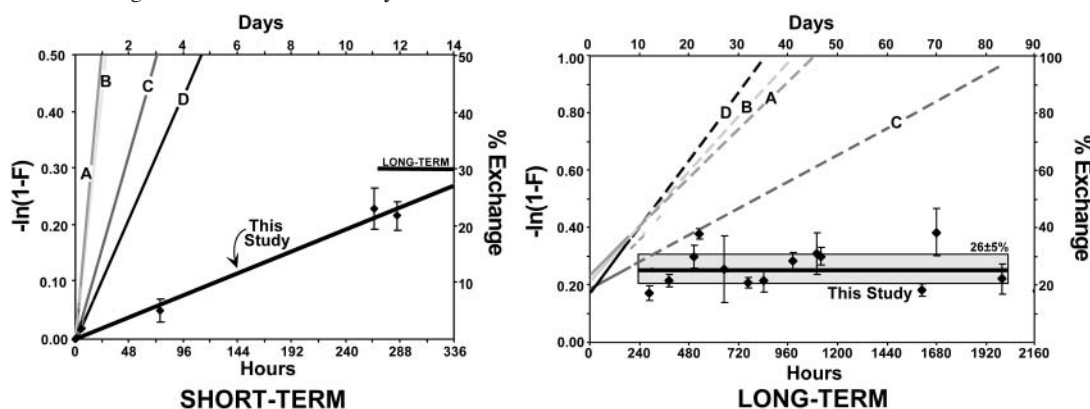


FIGURE 4. Plot of the percentage of Fe-isotope exchange vs. time for data from this study (Table 2) and that of Rea et al. (1994). Part A plots data for the first 12 days of this experiment, and part B the data for the 11–83 day duration of the experiment. The left y-axis for both figures recasts the proportion of Fe-isotope exchange (F) into a first-order rate law (see Johnson et al. 2002). Use of a second-order or zero-order rate law would not appreciably change the rate constants; a first-order rate law is preferred because it provides a better fit to the data within the constraint of an appropriate intercept (for a first-order rate law the intercept is 0). For the initial stages of this experiment (up to 12 days), the data are well fit by a first-order rate law with a rate constant of $0.00081 \pm 0.00003/\text{h}$ (error from least squares regression; $R^2 = 0.99$; intercept forced through 0). If data up to 22 days are used, the rate constant is identical within the given uncertainty. The long-term data are well fit by a horizontal line (regression of data indicate a rate constant of $0.000014 \pm 0.000030/\text{h}$ using data from 285 hours until the termination of the experiment). For comparison, the data for Fe-isotope exchange of Rea et al. (1994), as interpolated from best-fit lines, is shown by the curves labeled A (0.01 M NTA, Fh aged 1 week), B (0.01 M NTA, Fh aged 1 day), C (0.03 M NTA), and D (0.6 mM EDTA). In these experiments the Fe-isotope exchange data are best fit by two rate lines, an initial rapid exchange, followed by a slower exchange (see Table 3 for rate constants).

TABLE 3. Summary of rate constants for isotopic exchange

Solution	Short-term K_1	Long-term K_1	Reference
280 ppm Fe, 0.01 M NTA, pH=9, Ferrihydrite aged 1 d	0.0190/h	0.000840/h	Rea et al. (1994)
280 ppm Fe, 0.01 M NTA, pH=9, Ferrihydrite aged 1 wk	0.0198/h	0.000667/h	Rea et al. (1994)
280 ppm Fe, 0.03 M NTA, pH=9, Ferrihydrite aged 1 d	0.0068/h	0.000385/h	Rea et al. (1994)
280 ppm Fe, 0.6 mM EDTA, pH=9, Ferrihydrite aged 1 d	0.0045/h	0.001030/h	Rea et al. (1994)
0.1 ppm Fe, pH=4.7, stock 3 nm Ferrihydrite	0.0008/h	0.000014/h	This study

Notes: All rate constant are for a first-order rate law based on regression of Fe-isotope exchange data from this study and Rea et al. (1994). Short-term rate constants were fit to data <2 days for Rea et al. (1994), and <12 days from this study. Long-term rate constants were fit to data ≥ 2 days for Rea et al. (1994), and ≥ 12 days from this study (Fig. 4).

define a single line, with no discernible change in slope, we suggest that other mechanisms of isotopic exchange, such as isotopic exchange by “tunneling” along crystal defects or solid-state diffusion, are negligible. The relatively constant percentage of isotopic exchange from 11–83 days also indicates that no re-crystallization of the ferrihydrite has occurred, because re-crystallization would produce changes in the calculated percent of isotopic exchange through mobilization of Fe from the solid phase and accompanying isotopic communication with $\text{Fe(III)}_{\text{aq}}$ (e.g., Skulan et al. 2002; Johnson et al. 2004).

Our results are generally similar to those obtained by Rea et al. (1994), who used a radioactive ^{59}Fe tracer to investigate the kinetics of isotopic exchange between ferrihydrite and $\text{Fe(III)}_{\text{aq}}$, although the exchange rates they determined are several orders of magnitude faster than those measured in our experiments (Table 3). Rea et al. (1994) used nitrilotriacetic acid (NTA) and ethylenediaminetetraacetic acid (EDTA) as complexing ligands to increase aqueous Fe(III) contents to ensure sufficient ^{59}Fe abundances for the counting measurements. Rea et al. (1994) recognized the importance of conducting the isotopic exchange experiments at Fe solubility, and in their experiments, equilibrium $\text{Fe(III)}_{\text{aq}}$ contents ranged from 34–104 ppm, up to 1000 times higher than those used in our experiments that did not contain complexing ligands. Regression of the initial period of the experiments of Rea et al. (1994), assuming a first-order rate law, produces rate constants that are one to two orders of magnitude larger than those measured in our study (Table 3, Fig. 4).

The Fe-isotope exchange data of Rea et al. (1994) can be fit to two rate constants. In the initial stages of the experiment, there was rapid exchange, where rate constants were between 0.0045 to 0.0198/h (depending on the experimental conditions; Fig. 4). This rapid exchange accounted for approximately 20% isotope exchange. The initially rapid exchange was followed by slower exchange, where the rate constants varied between 0.000385 and 0.00103/h (depending on the experimental conditions; Fig. 4), which accompanied isotopic exchange between 20 and 30%. Rea et al. (1994) inferred that there were two distinct mechanisms of isotope exchange, where initial rapid exchange was interpreted to reflect exchange at labile ferrihydrite sites, and slower exchange was inferred to have occurred at non-labile sites, although mineralogical differences between the two sites were not defined. The slower exchange seems likely to reflect dissolution and re-precipitation of ferrihydrite. We note that dissolution and reprecipitation was the driving mechanism during the slow isotope exchange reactions that involved acid hydrolysis reactions between aqueous Fe(III) and hematite reported by Skulan et al. (2002).

In summary, our results document that complete isotopic

exchange occurs between $\text{Fe(III)}_{\text{aq}}$ and Fe in nanoparticulate ferrihydrite that lies in distorted “surface” sites on the order of 12 days in dilute aqueous solutions that are most closely analogous to natural environments. We find no evidence for isotopic exchange with the bulk crystal in dilute aqueous solutions. These results suggest that isotopic exchange in ferrihydrite will be strongly controlled by surface area and crystal size.

It is difficult to correlate the nanoparticulate ferrihydrite of this study directly with natural samples. The 3 nm ferrihydrite used probably represents a lower end-member case for particle size, although its measured surface area falls within the “normal” range commonly reported. Additionally, there was likely some undetermined amount of aggregation of the 3 nm particles over the experimental duration, perhaps increasing the similarity to natural larger samples. Until further experimental work of this nature is pursued using ferrihydrites of larger particle size, we cannot determine if the exchange observed in nanoparticulate ferrihydrite is consistent throughout larger size domains.

In an effort to be most conservative with our interpretation of Fe atom exchange measured in these experiments, we assume that Fe reactivity in ferrihydrite is primarily controlled by surface area, and that the 20–30% exchange observed in these experiments is in fact representative of exchange in individual 3 nm particles—providing a maximum for particle surface area relative to natural samples. For example, assuming a 2 Å surface layer (Fe-O bond length), which corresponds to ~35% surface Fe atoms for the 3 nm ferrihydrite used in this study, a 10 nm crystal would have only ~12% surface atoms. Natural ferrihydrite aggregates are generally 100 nm or more in diameter (Cornell and Schwertmann 1996), which, using the above parameters, would have only ~1% surface Fe atoms. Because isotopic exchange with the bulk crystal is essentially zero in dilute aqueous solutions (Fig. 4), nanoparticulate ferrihydrite that is larger than 100 nm may be considered isotopically inert in natural systems. In addition, because oxidation and precipitation rates in many natural systems such as terrestrial and marine hydrothermal systems occur over timescales of tens of minutes to several hours (e.g., Field and Sherrell 2000), even surface Fe sites in nm-size ferrihydrite should be isotopically inert.

ACKNOWLEDGMENTS

This work was supported by NSF grant EAR-0106614. We thank Walt Zeltner for performing the BET surface area analysis. Robert Nichols, Michael Hochella, and an anonymous reviewer provided journal reviews that were helpful in revising the manuscript. Thanks also to Sue Welch and Silke Severmann for their technical and intellectual assistance in the pursuit of this research.

REFERENCES CITED

Beard, B.L. and Johnson, C.M. (1999) High-precision Fe isotope compositions of lunar and terrestrial materials. *Geochimica et Cosmochimica Acta*, 63,

- 1653–1660.
- Beard, B.L., Johnson, C.M., Skulan, J.L., Neelson, K.H., Cox, L., and Sun, H. (2003) Application of Fe isotopes to tracing the geochemical and biological cycling of Fe. *Chemical Geology*, 195, 87–117.
- Cornell, R.M. and Schwertmann, U. (1996) *The Iron Oxides: Structure, Properties, Reactions, Occurrence and Uses*, 573 pp. VCH, Weinheim, Germany.
- Faure, G. (1986) *Principles of Isotope Geology*, 587 pp. Wiley, New York.
- Feng, Z., Zhao, J., Huggins, F.E., and Huffman, G.P. (1993) Agglomeration and phase transition of a nanophase iron oxide catalyst. *Journal of Catalysis*, 143, 510–519.
- Field, M.P., and Sherrell, R.M. (2000) Dissolved and particulate Fe in a hydrothermal plume at 9°45'N, East Pacific Rise: Slow Fe(II) oxidation kinetics in Pacific plumes. *Geochimica et Cosmochimica Acta*, 64, 619–628.
- Fox, L.E. (1988) The solubility of colloidal ferric hydroxide and its relevance to iron concentrations in river water. *Geochimica et Cosmochimica Acta*, 52, 771–777.
- Freer, R. and Hauptman, Z. (1978) An experimental study of magnetite-titanomagnetite interdiffusion. *Physics of the Earth and Planetary Interiors*, 16, 223–231.
- Ganguly, B., Huggins, F.E., Feng, Z., and Huffman, G.P. (1994) Anomalous recoilless fraction of 30-Å-diameter Fe-OOH particles. *Physical Review B*, 49, 3036–3042.
- Goldstein, A.N., Echer, C.M., and Alivisatos, A.P. (1992) Melting in semiconductor nanocrystals. *Science*, 256, 1425–1427.
- Ibrahim, M.M., Edwards, G., Seehra, M.S., Ganguly, B., and Huffman, G.P. (1994) Magnetism and spin dynamics of nanoscale FeOOH particles. *Journal of Applied Physics*, 75, 5873–5875.
- Ibrahim, M.M., Darwish, S., and Seehra, M.S. (1995) Nonlinear temperature variation of magnetic viscosity in nanoscale FeOOH particles. *Physical Review B*, 51, 2955–2959.
- Hochella, Jr. M.F. (2002) Nanoscience and technology: the next revolution in the Earth sciences. *Earth and Planetary Science Letters*, 203, 593–605.
- Johnson, C.M., Skulan, J.L., Beard, B.L., Sun, H., Neelson, K.H., and Braterman, P.S. (2002) Isotopic fractionation between Fe(III) and Fe(II) in aqueous solutions. *Earth and Planetary Science Letters*, 195, 141–153.
- Johnson, C.M., Beard, B.L., and Albarède, F. (2004) Overview and general concepts. In C.M. Johnson, B.L. Beard, and F. Albarède, Eds., *Geochemistry of non-traditional stable isotopes*, 55, 1–24. Reviews in Mineralogy and Geochemistry, Mineralogical Society of America, Washington, D.C.
- Manceau, A. and Gates, W.P. (1997) Surface structural model for ferrihydrite. *Clays Clay Minerals*, 45, 448–460.
- Rea, B.A., Davis, J.A., and Waychunas, G.A. (1994) Studies of the reactivity of the ferrihydrite surface by iron isotopic exchange and Mossbauer spectroscopy. *Clays and Clay Minerals*, 42, 23–34.
- Skulan, J.L., Beard, B.L., and Johnson, C.M. (2002) Kinetic and equilibrium Fe isotope fractionation between aqueous Fe(III) and hematite. *Geochimica et Cosmochimica Acta*, 66, 2995–3015.
- Stipp, S.L.S., Hansen, M., Kristensen, R., Hochella Jr., M.F., Bennedsen, L., Dideriksen, K., Balic-Zunic, T., Leonard, D., and Mathieu, H.-J. (2002) Behavior of Fe-oxides relevant to contaminant uptake in the environment. *Chemical Geology*, 190, 321–337.
- Stookey, L.L. (1970) *Ferrozine*—a new spectrophotometric reagent for iron. *Analytical Chemistry*, 42, 779–781.
- Tolbert, S.H. and Alivisatos, A.P. (1995) High-pressure structural transformations in semiconductor nanocrystals. *Annual Reviews in Physical Chemistry*, 46, 595–625.
- Trudeau, M.L. and Ying, J.Y. (1996) Nanocrystalline materials in catalysis and electrocatalysis: structure tailoring and surface reactivity. *NanoStructured Materials*, 7, 245–258.
- Waychunas, G.A. (2001) Structure, aggregation, and characterization of nanoparticles. In J.F. Banfield and A. Navrotsky, Eds., *Nanoparticles and the Environment*, 44, 105–162. Reviews in Mineralogy and Geochemistry, Mineralogical Society of America, Washington, D.C.
- Zhao, J., Huggins, F.E., Feng, Z., Lu, F., Shah, N., and Huffman, G.P. (1993) Structure of a nanophase iron oxide catalyst. *Journal of Catalysis*, 143, 499–509.
- Zhao, J., Huggins, F.E., Feng, Z., and Huffman, G.P. (1994) Ferrihydrite: surface structure and its effects on phase transformation. *Clays and Clay Minerals*, 42, 737–746.

MANUSCRIPT RECEIVED SEPTEMBER 1, 2004

MANUSCRIPT ACCEPTED NOVEMBER 3, 2004

MANUSCRIPT HANDLED BY ROBERT F. DYMEK